

# CROSS SECTION RATIOS BETWEEN DIFFERENT CM ENERGIES AT THE LHC: OPPORTUNITIES FOR PRECISION MEASUREMENTS AND BSM SENSITIVITY

Michelangelo L. Mangano<sup>a</sup> and Juan Rojo<sup>a</sup>

<sup>a</sup> PH Department, TH Unit, CERN, CH-1211 Geneva 23, Switzerland

E-mail: michelangelo.mangano@cern.ch, juan.rojo@cern.ch

November 8, 2018

## Abstract

The staged increase of the LHC beam energy provides a new class of interesting observables, namely ratios and double ratios of cross sections of various hard processes. The large degree of correlation of theoretical systematics in the cross section calculations at different energies leads to highly precise predictions for such ratios. We present in this letter few examples of such ratios, and discuss their possible implications, both in terms of opportunities for precision measurements and in terms of sensitivity to Beyond the Standard Model dynamics.

# 1 Introduction

The excellent performance of the LHC accelerator complex and of the experiments has allowed, in just a matter of a couple of years, for very precise cross section measurements covering a broad range of hard final states, such as jets [1–3], top quarks [4–8], electroweak gauge bosons [9–14], direct photons [15,16], and associated production thereof [17–19]. When these results are compared to the available precise theoretical calculations [20], improved information can be inferred on the structure of the proton [21,22] and of the Standard Model (SM) parameters, and indications of possible departures from the SM itself can be detected. Given the rich statistics of the LHC data, this programme is typically limited in its potential only by the nature and size of the systematic uncertainties that accompany both the measurements and the theoretical calculations. To the extent that such uncertainties can be correlated among different processes, it is possible to define combinations of various observables that can be calculated, and possibly measured, with a higher degree of precision.

Several works in the past have already introduced key ideas to define a programme of precision cross section measurements at the LHC. For example, refs. [23–25] introduced and explored the use of precisely known Drell-Yan and QED processes to extract indirectly the absolute LHC luminosity, and to correlate the PDF systematics in cross sections of different processes. More recently, refs. [26,27] discussed the precision and discovery potential of comparing rate measurements performed at different beam energies, and with different beam types.

The goal of this letter is to provide an up-to-date quantitative estimate to the intrinsic theoretical precision of ratios and double ratios of cross sections for different processes, measured at different beam energies, using the most accurate perturbative knowledge and the latest PDF sets. We focus on observables that are already routinely measured by the LHC detectors, and for which the performance has been established. Depending on which ratios one is willing to take from theory as benchmarks, this precision can be used to correlate luminosity measurements at different energies, to validate experimental measurements of specific cross sections, to test and improve PDF fits, and even to probe the existence of underlying BSM phenomena.

A typical example of the quantities that have been discussed in the literature is the ratio of the cross section for a given process  $X$  by the production rate of  $Z$  bosons. The latter is the most precisely determined rate in hadronic collisions, both theoretically and experimentally. Rescaling the rate of  $X$  to the  $Z$  cross section removes entirely the experimental uncertainty on the LHC luminosity, and could also lead to a further reduction of the theoretical sensitivity to the parton density functions (PDFs) that parametrize the proton quark and gluon structure. This is true, for example, of the ratios  $\sigma(Z + \text{jet})/\sigma(Z)$ , or  $\sigma(W)/\sigma(Z)$ . However, the theoretical systematics, such as the scale uncertainty, are generally totally uncorrelated between the process  $X$  and  $Z$  production, and cannot be reduced by taking this ratio.

In this letter we explore the nature of the correlations among theoretical systematics, and the precision potential, of measurements taken at different LHC beam energies. This is motivated by the staged approach of the LHC to higher energies, with large sets accumulated, so far, at  $\sqrt{s} = 7$  TeV, and expected this year at  $\sqrt{s} = 8$  TeV, and following 2014 at  $\sqrt{s} \sim 14$  TeV.

The key observation is that, for a given process, the calculation of cross sections at different energies requires correlated values of the various input parameters, such as masses,  $\alpha_S$ , PDFs and scales. When these parameters are varied simultaneously at the two energies, the cross section ratio is much less sensitive to their variation. When comparing this prediction to data, three things can happen:

- if the residual theoretical systematics is dominated by PDFs (as will be the case in several of the examples shown below), and is larger than the achievable experimental precision, the data versus theory comparison can be used to improve the PDF determination;
- the theoretical systematics could be small enough that, with a comparable experimental precision, the measurement becomes sensitive to possible contributions from physics beyond the SM

(BSM);

- when residual systematic errors are small enough, and no BSM contribution is within reach, one can use the cross section ratios as standard candles for luminosity measurement and cross calibration; for example, to correlate the luminosity measurement between two beam energies and between two different experiments.

In all cases, the improved theoretical precision provides the experiments with an important diagnostic tool for the validation of the analyses at different energies, and a benchmark to be used for a possible reduction of some of the experimental uncertainties.

We give in this paper a few examples to illustrate the above points. Several other cases of interest can be considered, but a conclusive assessment of whether these proposals are indeed useful will require an in-depth analysis of the challenge posed by correlating the experimental systematics at different energies. Experimental cross section systematics typically fall in three categories: efficiencies/acceptances, energy scales and absolute luminosity. The first arises from a mixture of purely experimental effects and theoretical modeling: in the case of leptonic final states, such as  $W$  or  $Z$  bosons measurements, these uncertainties can be brought to a (sub)percent level, and further reduced in ratios. In the case of jets, the energy scales dominate the uncertainties, at the level of up to 10-20 %. While the event structure varies at different CM energies and running conditions (e.g. due to pile-up of multiple  $pp$  interactions), it is likely that a large fraction of these systematics can be correlated.

The direct measurement of the LHC absolute luminosity has improved significantly over the last year, and is now estimated to attain the level of 2%, a systematics which is however uncorrelated among different CM energies [28]. The simultaneous measurement of total  $pp$  cross section and luminosity, at the level of few percent, can be obtained, by using the optical theorem, by the TOTEM [29, 30] and ALFA [31] detectors. New detector concepts have been proposed [26, 32, 33], capable of measuring and fully exploiting the precisely known cross section for exclusive electromagnetic production of dilepton pairs ( $pp \rightarrow pp\ell^+\ell^-$ ) [24, 34, 35]. These could improve the absolute luminosity measurement to 1%, and the relative luminosity at different energies, and for different hadronic beam types, to 0.1% [26]. Nevertheless, the only way to further reduce the luminosity uncertainty in the ongoing runs, in fact to fully remove it, is to take cross-section ratios for different processes.

The outline of this letter is as follows. On Sect. 2 we provide more details on the theoretical framework for our calculations and present explicit quantitative results relative to production of electroweak gauge bosons, top quarks, Higgs boson and jets. Then in Sect. 3 we discuss how to understand the generic dependence of cross section ratios in terms of ratios of PDF luminosities. In Sect. 4 we discuss how the possible sensitivity to BSM contributions might be enhanced in cross section ratios, and then we conclude.

## 2 Theoretical systematic errors in cross section ratios

The main focus of the present paper will be the ratio of cross sections for a final state  $X$  between different LHC center of mass energies  $E_{1,2} = \sqrt{s_{1,2}}$ :

$$R_{E_2/E_1}(X) \equiv \frac{\sigma(X, E_2)}{\sigma(X, E_1)}, \quad (1)$$

with  $E_i = 7, 8$  or  $14$  TeV.<sup>1</sup> In view of the cancellation of the luminosity, we shall also consider double ratios of cross sections:

$$R_{E_2/E_1}(X, Y) \equiv \frac{\sigma(X, E_2)/\sigma(Y, E_2)}{\sigma(X, E_1)/\sigma(Y, E_1)} \equiv \frac{R_{E_2/E_1}(X)}{R_{E_2/E_1}(Y)}. \quad (2)$$

---

<sup>1</sup>There is also data at  $\sqrt{s} = 2.76$  TeV, used mostly for  $pp$  benchmarks in  $PbPb$  measurements, but experimental uncertainties are larger and thus we will not consider this case here.

In this work we consider two classes of observables. First of all we consider inclusive cross sections for electroweak gauge boson production, top quark pair production, and Higgs boson production in the gluon fusion channel. Next, we consider more differential distributions, in particular the top quark pair cross section above a certain threshold in the invariant mass of the  $t\bar{t}$  pair and inclusive jet production in a given range of  $p_T$  and rapidity. For each of these processes we have evaluated all the relevant associated systematic theoretical uncertainties due to:

- Parton Distribution Functions
- Higher perturbative orders
- Values of  $m_t$  and  $\alpha_s(M_Z)$

To be more precise, we have used the following codes and settings for cross section computations:

- Electroweak gauge boson production has been computed at NNLO using the **Vrap** code [36]. The central scale is  $Q^2 = M_V^2$ .
- Top quark pair production has been computed at NLO+NNLL with the **top++** code [37]<sup>2</sup>. The central scale is  $Q^2 = m_t^2$ . The settings of the theoretical calculations are the default ones in Ref. [39].
- Higgs boson production cross sections in the gluon fusion channel have been computed at NNLO with the **iHixs** code [40]. The central scale has been taken to be  $Q = M_H/2$ , to simulate the effects of NNLL resummation [41].
- Top quark pair production with a lower cut on the top-antitop quark pair invariant mass of 1 TeV and 2 TeV has been computed at NLO with the **MCFM6.2** code [42, 43], and cross-checked with the **MNR** code [44]. The central scale has been taken to be  $Q^2 = M_{t\bar{t}}^2$ , the invariant mass of the top-antitop pair. This is a suitable choice of scale since it is of the same order of magnitude of the typical hard scales involved in these processes. We verified that the scale systematics for cross section ratios is consistent with the alternative choice of  $Q^2 = m_t^2 + \langle p_T^2 \rangle$ , where  $\langle p_T^2 \rangle = (p_{T,t}^2 + p_{T,\bar{t}}^2)/2$ .
- Inclusive jet production with a lower cut in the transverse momentum of the jet of 1 TeV and 2 TeV in the region  $|\eta| \leq 2.5$  has been computed at NLO with a modified version of the **EKS** jet production program [45]. The calculation uses the anti- $k_T$  algorithm with  $R = 0.6$ , with the scale in each event set equal to the  $p_T$  of the hardest jet in the event. As cross-checks, we have also computed inclusive jet cross sections with the **FastNLO** program [46, 47], based on **NLOjet++** [48], for 7 and 8 TeV, for a fine binning in the transverse momentum of the jet and in the central region with  $|\eta| \leq 0.5$ .

The choice of PDF sets, and the values of the SM parameters and the calculation of theoretical systematics adopted in our computation are the following:

- The reference PDF set is the NNPDF2.1 NNLO set [49, 50]. For cross-checks, and to gauge the sensitivity with respect the choice of PDF set, we will use in addition the MSTW2008nnlo [51] and ABKM09 NNLO [52] PDF sets.
- For all processes, renormalization and factorization scales have been varied in the range  $0.5 \leq \mu_R/Q, \mu_F/Q \leq 2$ , with the constraint that  $0.5 \leq \mu_R/\mu_F \leq 2$ , to avoid artificial large logarithms of scale ratios. For ratios of different observables, scale variations in the numerator and in the

---

<sup>2</sup>We did not include the latest development of the calculation of the complete NNLO corrections to the  $q\bar{q} \rightarrow t\bar{t}$  production, documented in [38]. Their effect would be to further reduce slightly the theoretical scale systematics.

Cross Section	$R^{\text{th,nnpdf}}$	$\delta_{\text{PDF}}(\%)$	$\delta_{\alpha_s}(\%)$	$\delta_{\text{scales}}(\%)$
$t\bar{t}/Z$	1.23	$\pm 0.4$	$-0.2 - 0.2$	$-0.2 - 0.3$
$t\bar{t}$	1.43	$\pm 0.3$	$-0.2 - 0.2$	$-0.1 - 0.3$
$Z$	1.16	$\pm 0.1$	$-0.0 - 0.1$	$-0.1 - 0.1$
$W^+$	1.15	$\pm 0.1$	$-0.0 - 0.1$	$-0.1 - 0.1$
$W^-$	1.17	$\pm 0.1$	$-0.0 - 0.1$	$-0.1 - 0.1$
$W^+/W^-$	0.98	$\pm 0.1$	$-0.0 - 0.0$	$-0.0 - 0.0$
$W/Z$	0.99	$\pm 0.0$	$-0.0 - 0.0$	$-0.0 - 0.0$
$ggH$	1.27	$\pm 0.2$	$-0.0 - 0.1$	$-0.2 - 0.2$
$t\bar{t}(M_{t\bar{t}} \geq 1 \text{ TeV})$	1.81	$\pm 0.8$	$-0.0 - 0.3$	$-0.6 - 0.5$
$t\bar{t}(M_{t\bar{t}} \geq 2 \text{ TeV})$	2.80	$\pm 3.2$	$-0.6 - 0.3$	$-0.0 - 1.4$
$\sigma_{\text{jet}}(p_T \geq 1 \text{ TeV})$	2.30	$\pm 1.0$	$-0.0 - 0.5$	$-0.4 - 1.0$
$\sigma_{\text{jet}}(p_T \geq 2 \text{ TeV})$	7.38	$\pm 5.2$	$-0.4 - 1.0$	$-2.5 - 2.3$

Table 1: For each observable listed in the first column, the second column shows the theoretical expectation of the ratio  $R^{\text{th}}$  between 8 and 7 TeV, computed with NNPDF2.1, and then the relevant systematic theoretical uncertainties: PDFs,  $\alpha_s$  and scale variation, computed as discussed in the text. The theory systematics are given as percentage with respect to the central prediction. In some cases the theory systematics in the cross section ratios is at the sub-permille level, this is indicated as 0.0 in the tables.

denominator are taken as uncorrelated, and thus added in quadrature, except for  $W$  and  $Z$  ratios where scale variations are taken as fully correlated between numerator and denominator. The scale uncertainty  $\delta_{\text{scale}}$  is defined as the maximum (minimum) difference between the result at the central scale and the results varying the scales in the above range.

- PDF uncertainties are computed directly on the cross section ratios, keeping track of all the PDF induced correlations between numerator and denominator.
- The reference value for the strong coupling has been taken to be  $\alpha_s(M_Z^2) = 0.119$ , and a conservative uncertainty of  $\delta_{\alpha_s} = 0.002$  at the 68% CL is assumed [53]. The correlations between PDFs and  $\alpha_s$  are consistently taken into account, using the NNPDF sets with varying  $\alpha_s$  as described in [54, 55]
- The reference value of the top quark mass is taken to be  $m_t = 173.3 \text{ GeV}$  [56], with a conservative uncertainty of  $\delta_{m_t} = 2 \text{ GeV}$ . We have verified that the dependence of the cross section ratios on the top quark mass is very small, for example for the 8 over 7 TeV ratio it is at most 1 permille, much smaller than any other theory systematics, and this is the same for all other cases studied. Therefore in the following we will not provide the explicit contribution of  $\delta_{m_t}$  to the total theory systematics, since is always negligible as compared to PDF, scale and  $\alpha_s$  uncertainties.
- We assume a Standard Model Higgs with mass  $m_H = 125 \text{ GeV}$ . We verified that the impact on our results of a possible  $\delta_{m_H} = 2 \text{ GeV}$  uncertainty on its mass is negligible.

We have collected the results for cross section ratios between 8 and 7 TeV, 14 and 7 TeV, and 14 and 8 TeV, in Tables 1–3. For each process  $X$  (or ratio of processes  $X$  and  $Y$ ) we show the theoretical expectation for  $R^{\text{th}}(X)$  ( $R^{\text{th}}(X, Y)$ ) and the relevant systematic theoretical uncertainties: PDFs, strong coupling and scales. We then studied the stability of our results with respect to changes in the PDF parameterizations, as shown in Tables 4–6, where we collect the central values, systematics and shifts relative to the reference NNPDF2.1 NNLO set, obtained by using the MSTW08 and ABKM09 NNLO PDF sets. Using different PDFs is important to assess the robustness of the theory prediction, since in some cases differences among PDF sets differ by a larger amount than the nominal PDF uncertainty of each set. The results for a representative subset of these cross section ratios obtained with different PDF sets are also represented graphically in Fig. 1.

We summarize here the main features of these results. Let us focus first on the results for  $R_{8/7}$ :

Cross Section	$R^{\text{th,nnpdf}}$	$\delta_{\text{PDF}}(\%)$	$\delta_{\alpha_s}(\%)$	$\delta_{\text{scales}}(\%)$
$t\bar{t}/Z$	2.61	$\pm 1.6$	$-1.1 - 1.0$	$-0.6 - 1.4$
$t\bar{t}$	5.58	$\pm 1.4$	$-0.7 - 0.9$	$-0.5 - 1.4$
$Z$	2.14	$\pm 0.8$	$-0.1 - 0.4$	$-0.3 - 0.3$
$W^+$	2.01	$\pm 0.8$	$-0.0 - 0.3$	$-0.4 - 0.3$
$W^-$	2.17	$\pm 0.8$	$-0.1 - 0.3$	$-0.4 - 0.2$
$W^+/W^-$	0.93	$\pm 0.4$	$-0.0 - 0.1$	$-0.0 - 0.1$
$W/Z$	0.97	$\pm 0.2$	$-0.1 - 0.1$	$-0.0 - 0.0$
$ggH$	3.26	$\pm 0.8$	$-0.1 - 0.2$	$-1.1 - 1.1$
$t\bar{t}(M_{t\bar{t}} \geq 1 \text{ TeV})$	14.8	$\pm 3.3$	$-1.0 - 1.2$	$-2.2 - 2.6$
$t\bar{t}(M_{t\bar{t}} \geq 2 \text{ TeV})$	69.7	$\pm 9.6$	$-0.6 - 0.6$	$-2.8 - 2.0$
$\sigma_{\text{jet}}(p_T \geq 1 \text{ TeV})$	34.9	$\pm 2.9$	$-0.0 - 0.3$	$-2.0 - 2.8$
$\sigma_{\text{jet}}(p_T \geq 2 \text{ TeV})$	1340	$\pm 12$	$-0.7 - 1.1$	$-8.0 - 6.4$

Table 2: Same as Table 1 for ratios between 14 and 7 TeV LHC center of mass energies.

Cross Section	$R^{\text{th,nnpdf}}$	$\delta_{\text{PDF}}(\%)$	$\delta_{\alpha_s}(\%)$	$\delta_{\text{scales}}(\%)$
$t\bar{t}/Z$	2.12	$\pm 1.3$	$-0.8 - 0.8$	$-0.4 - 1.1$
$t\bar{t}$	3.90	$\pm 1.1$	$-0.5 - 0.7$	$-0.4 - 1.1$
$Z$	1.84	$\pm 0.7$	$-0.1 - 0.3$	$-0.3 - 0.2$
$W^+$	1.75	$\pm 0.7$	$-0.0 - 0.3$	$-0.3 - 0.2$
$W^-$	1.86	$\pm 0.6$	$-0.1 - 0.3$	$-0.3 - 0.1$
$W^+/W^-$	0.94	$\pm 0.3$	$-0.0 - 0.0$	$-0.0 - 0.0$
$W/Z$	0.98	$\pm 0.1$	$-0.1 - 0.0$	$-0.0 - 0.0$
$ggH$	2.56	$\pm 0.6$	$-0.1 - 0.1$	$-0.9 - 1.0$
$t\bar{t}(M_{t\bar{t}} \geq 1 \text{ TeV})$	8.18	$\pm 2.5$	$-1.3 - 1.1$	$-1.6 - 2.1$
$t\bar{t}(M_{t\bar{t}} \geq 2 \text{ TeV})$	24.9	$\pm 6.3$	$-0.0 - 0.3$	$-3.0 - 1.1$
$\sigma_{\text{jet}}(p_T \geq 1 \text{ TeV})$	15.1	$\pm 2.1$	$-0.4 - 0.0$	$-1.9 - 2.4$
$\sigma_{\text{jet}}(p_T \geq 2 \text{ TeV})$	182	$\pm 7.7$	$-0.3 - 0.2$	$-5.7 - 4.0$

Table 3: Same as Table 1 for ratios between 14 and 8 TeV LHC center of mass energies.

- For  $W$  and  $Z$  production processes, all sources of uncertainties have a comparable size, typically of  $\mathcal{O}(10^{-3})$  or below. The  $W^-$  ratios obtained with the ABKM09 set differ from NNPDF2.1 and MSTW08 by  $2.3 \times 10^{-3}$ , which is nominally a difference of about  $2\sigma$ , given the individual values of  $\delta_{\text{PDF}}$ . This difference however is much reduced when considering double ratios ( $W^+/W^-$  and  $Z/W$ ), and therefore it is unlikely to be measurable, given the uncertainty on the relative luminosity calibration at the two energies, which is  $\sim 2\%$ . Notice nevertheless that, since the stability of single ratios, for all PDF sets, is at the level of  $\sim 2 \times 10^{-3}$ , a precise measurement of  $R(Z)$  or  $R(W)$  can correlate the luminosities of runs at the two energies with this level of accuracy.
- For inclusive  $t\bar{t}$  production, and for both  $R(t\bar{t})$  and  $R(t\bar{t}, Z)$ ,  $\delta_{\text{scale}} \oplus \delta_{\alpha_s} \sim 4 \times 10^{-3}$ . The difference between NNPDF2.1 and MSTW08, as well as the individual  $\delta_{\text{PDF}}$ , are of similar size, while a shift slightly larger than 1% is observed with respect to ABKM09. This corresponds to a  $\sim 2.5\sigma$  change, thus a potential probe of the gluon PDF parameterizations.
- For  $t\bar{t}$  production at large mass,  $\delta_{\text{scale}} \sim 1\%$ , while  $\delta_{\text{PDF}}$  is of the order of several %, consistent with the intrinsic differences among the different PDF sets.  $R(t\bar{t})$  provides therefore a useful constraint for the gluon density at large  $x$  (see the discussion of the initial-state composition in  $t\bar{t}$  events, in Sect. 4, where we show that high mass  $t\bar{t}$  production is dominated by the  $gg$  process).
- In the case of the jet rates, the scale uncertainty is comparable to the PDF one for  $p_T > 1 \text{ TeV}$ , while the PDF uncertainty dominates when  $p_T > 2 \text{ TeV}$ . This suggest that ratios of high- $p_T$



jet cross sections could be useful to constrain large- $x$  quark PDFs. To study this possibility in more detail, we have cross-checked the jet theory systematics in the 8 over 7 TeV cross section ratios using **FastNLO** with a finer binning of  $p_T$  and rapidity. In Fig. 2 we show the PDF and scale systematics for LHC inclusive jet production as a function of the  $p_T$  of the jet, in the central region  $|\eta| \leq 0.5$ . As can be seen, PDF and scale systematics are below 1% below 1 TeV, and while scale systematics are small even for larger  $p_T$ , at some point near  $p_T \sim 2.5$  TeV (corresponding to a final state with approximately  $m_X \sim 5$  TeV in the central region) the PDF uncertainties blow up: therefore, measurements in this region would be important to constrain large- $x$  PDFs.

Considering the ratios at 14 and 8 TeV, the following additional remarks can be made:

- For electroweak processes, all uncertainties grow slightly, but still remain well below 1% in the case of NNPDF2.1 and MSTW08. Rate ratios obtained with ABKM09 are about 1% smaller, which is a  $\sim 2\sigma$  effect. Once again, the measurement of these ratios provides a very effective tool to calibrate at the percent level the relative normalization of the 8 TeV and 14 TeV absolute luminosities.
- For  $R(t\bar{t})$ , the scale systematics is  $\sim 1\%$ . As in the case of the 8/7 ratios, PDF differences between NNPDF2.1 and MSTW08 are compatible with the individual values of  $\delta_{\text{PDF}}$ , which are also  $\sim 1\%$ . The value of  $R(t\bar{t})$  obtained with ABKM09 is  $\sim 5\%$  smaller, corresponding to a  $\sim 2.5\sigma$  effect.
- For  $t\bar{t}$  production at large mass,  $\delta_{\text{scale}} \sim 2 - 3\%$ , while  $\delta_{\text{PDF}}$  grows to 6%, showing a great sensitivity to the PDF distributions.
- The gluon fusion Higgs production cross sections has very small PDF and scale systematics in the 14 over 8 TeV ratio. Therefore, measurements of this ratio could provide stringent tests of the hypothesis that the measured Higgs boson indeed behaves as a Standard Model Higgs boson from the production point of view. As suggested in [27], consideration of rate ratios for individual Higgs decay final states (e.g.  $WW^* \rightarrow 2\ell 2\nu$ ) could also be used to consolidate the separation of signal and backgrounds, due to the different energy scaling of the respective rates.
- Scale and PDF uncertainties are comparable in the case of jet production, for both thresholds of  $p_T > 1$  TeV and  $p_T > 2$  TeV. This is the result of the rather different composition of the initial state at the two energies (see Sect. 4), so that the scale dependence at the two energies is only weakly correlated.

### 3 Parton luminosity ratios

In order to understand better the behavior of cross section ratios and their PDF systematics presented in the previous section, as well as to maximize the sensitivity to BSM effects, it is useful to consider parton-parton luminosities [57]. Parton luminosities encode the essential information from the partonic contribution for different subprocesses. We define four different parton luminosities:<sup>3</sup>

- Gluon-Gluon luminosity:

$$\mathcal{L}_{gg}(M, s) \equiv \frac{1}{s} \int_{\tau}^1 \frac{dx}{x} g(x, M) g(\tau/x, M) \quad (3)$$

---

<sup>3</sup>One can define other partonic luminosities for more specific processes, like the  $bg$  luminosity, but the four that we discuss are enough for the most important processes.

Ratio	$R^{\text{nnpdf}}$	$\delta_{\text{PDF}}(\%)$	$R^{\text{mstw}}$	$\delta_{\text{PDF}}(\%)$	$\Delta^{\text{mstw}}(\%)$	$R^{\text{abkm}}$	$\delta_{\text{abkm}}(\%)$	$\Delta^{\text{abkm}}(\%)$
$t\bar{t}/Z$	1.23	0.4	1.23	0.2	+0.3	1.25	0.5	-1.3
$t\bar{t}$	1.43	0.3	1.43	0.2	+0.3	1.45	0.5	-1.4
$Z$	1.16	0.1	1.16	0.1	+0.0	1.16	0.1	-0.1
$W^+$	1.15	0.1	1.15	0.1	-0.1	1.15	0.1	-0.2
$W^-$	1.17	0.1	1.17	0.1	+0.0	1.17	0.1	-0.2
$W^+/W^-$	0.98	0.1	0.98	0.0	-0.1	0.98	0.0	+0.0
$W/Z$	0.99	0.0	0.99	0.0	-0.0	0.99	0.0	+0.0
$ggH$	1.27	0.2	1.27	0.2	-0.1	1.24	0.2	+2.6
$t\bar{t}(M_{t\bar{t}} \geq 1 \text{ TeV})$	1.81	0.8	1.79	0.7	+0.9	1.86	1.0	-2.7
$t\bar{t}(M_{t\bar{t}} \geq 2 \text{ TeV})$	2.80	3.2	2.64	2.8	+5.7	2.74	5.2	+2.3
$\sigma_{\text{jet}}(p_T \geq 1 \text{ TeV})$	2.30	1.0	2.29	2.2	+0.3	2.27	2.0	+1.1
$\sigma_{\text{jet}}(p_T \geq 2 \text{ TeV})$	7.38	5.2	7.77	3.1	-4.5	7.69	4.9	-3.5

Table 4: For each observable listed in the first column, we show the theoretical predictions for the various observables ratios between 8 and 7 TeV when computing with the NNPDF2.1, MSTW08 and ABKM09 NNLO PDF sets, as well as the respective percentage PDF error  $\delta_{\text{PDF}}$  in each case and the percentage shift with respect the NNPDF2.1 prediction. When the shift with respect to NNPDF2.1 is below the permille level it is denoted by 0.0 in the table. In each case the default value of  $\alpha_s(M_Z)$  provided by MSTW08 ( $\alpha_s(M_Z) = 0.1171$ ) and ABKM09 ( $\alpha_s(M_Z) = 0.1135$ ) have been used. to be compared with  $\alpha_s(M_Z) = 0.119$  in the baseline NNPDF2.1 predictions.

Ratio	$R^{\text{nnpdf}}$	$\delta_{\text{PDF}}(\%)$	$R^{\text{mstw}}$	$\delta_{\text{PDF}}(\%)$	$\Delta^{\text{mstw}}(\%)$	$R^{\text{abkm}}$	$\delta_{\text{abkm}}(\%)$	$\Delta^{\text{abkm}}(\%)$
$t\bar{t}/Z$	2.61	1.6	2.59	1.2	+0.9	2.76	2.4	-5.6
$t\bar{t}$	5.58	1.4	5.53	1.2	+1.0	5.96	2.4	-6.7
$Z$	2.14	0.8	2.14	0.5	+0.1	2.16	0.4	-1.0
$W^+$	2.01	0.8	2.01	0.6	-0.1	2.03	0.4	-1.2
$W^-$	2.17	0.8	2.16	0.5	+0.3	2.20	0.4	-1.3
$W^+/W^-$	0.93	0.4	0.93	0.2	-0.4	0.92	0.2	+0.1
$W/Z$	0.97	0.2	0.97	0.1	-0.0	0.97	0.1	-0.2
$ggH$	3.26	0.8	3.28	0.7	-0.4	3.28	0.8	-0.4
$t\bar{t}(M_{t\bar{t}} \geq 1 \text{ TeV})$	14.8	3.3	14.3	2.3	+3.3	16.6	4.1	-12.5
$t\bar{t}(M_{t\bar{t}} \geq 2 \text{ TeV})$	69.7	9.6	61.7	6.0	+11.9	75.4	10.1	-7.6
$\sigma_{\text{jet}}(p_T \geq 1 \text{ TeV})$	34.9	2.9	34.8	2.1	-0.2	33.6	2.2	+3.1
$\sigma_{\text{jet}}(p_T \geq 2 \text{ TeV})$	1340	12.4	1527	4.0	-11.5	1344	6.2	+1.8

Table 5: Same as Table 4 but for cross section ratios between 14 and 7 TeV.

- Quark-Gluon luminosity

$$\begin{aligned}
\mathcal{L}_{gq}(M, s) \equiv & \frac{1}{s} \int_{\tau}^1 \frac{dx}{x} \sum_{i=1}^{n_f} \left[ g(x, M) (q_i(\tau/x, M) + \bar{q}_i(\tau/x, M)) \right. \\
& \left. + (q_i(x, M) + \bar{q}_i(x, M)) g(\tau/x, M) \right]
\end{aligned} \tag{4}$$

- Quark-Antiquark luminosity

$$\mathcal{L}_{q\bar{q}}(M, s) \equiv \frac{1}{s} \int_{\tau}^1 \frac{dx}{x} \left[ \sum_{i,j=1}^{n_f} (q_i(x, M) \bar{q}_j(\tau/x, M) + \bar{q}_i(x, M) q_j(\tau/x, M)) \right] \tag{5}$$

- Quark-Quark luminosity

$$\mathcal{L}_{qq}(M, s) \equiv \frac{1}{s} \int_{\tau}^1 \frac{dx}{x} \left[ \sum_{i,j=1}^{n_f} q_i(x, M) q_j(\tau/x, M) \right] \tag{6}$$

In the above definitions,  $\tau = M^2/s$ ,  $M$  is the invariant mass of the produced final state and  $\sqrt{s}$  is the hadronic center of mass energy. Also  $n_f$  is the number of active quark flavors at scale  $M$ . This



Ratio	$R^{\text{nnpdf}}$	$\delta_{\text{PDF}}(\%)$	$R^{\text{mstw}}$	$\delta_{\text{PDF}}(\%)$	$\Delta^{\text{mstw}}(\%)$	$R^{\text{abkm}}$	$\delta_{\text{abkm}}(\%)$	$\Delta^{\text{abkm}}(\%)$
$t\bar{t}/Z$	2.12	1.3	2.11	0.9	+0.6	2.21	1.9	-4.3
$t\bar{t}$	3.90	1.1	3.87	0.9	+0.7	4.10	1.9	-5.2
$Z$	1.84	0.7	1.84	0.4	+0.1	1.85	0.3	-0.8
$W^+$	1.75	0.7	1.75	0.5	+0.0	1.77	0.3	-1.0
$W^-$	1.86	0.6	1.85	0.4	+0.3	1.88	0.3	-1.1
$W^+/W^-$	0.94	0.3	0.94	0.2	-0.3	0.94	0.1	+0.0
$W/Z$	0.98	0.1	0.98	0.1	+0.0	0.98	0.1	-0.2
$ggH$	2.56	0.6	2.57	0.6	+0.3	2.64	0.7	-3.1
$t\bar{t}(M_{t\bar{t}} \geq 1 \text{ TeV})$	8.18	2.5	7.99	2.0	+2.5	8.97	3.6	-9.6
$t\bar{t}(M_{t\bar{t}} \geq 2 \text{ TeV})$	24.9	6.3	23.3	4.3	+6.4	27.5	6.2	-10.3
$\sigma_{\text{jet}}(p_T \geq 1 \text{ TeV})$	15.1	2.1	15.2	1.9	-0.5	14.8	1.8	+1.9
$\sigma_{\text{jet}}(p_T \geq 2 \text{ TeV})$	181.6	7.7	196.4	3.3	-7.1	174.7	4.9	+4.7

Table 6: Same as Table 4 but for cross section ratios between 14 and 8 TeV.

definition includes the contribution of the top quark PDFs, but we have verified that PDF luminosities defined for a  $n_f = 5$  scheme (where top is always considered a massive parton) are very similar in the relevant kinematical region.

Of particular interest in our case are the ratios of parton luminosities between different LHC center of mass energies. For the time being we concentrate on 14 over 8 TeV ratios and 8 over 7 TeV ratios, the most relevant ones from the phenomenological point of view. These PDF luminosity ratios are defined as:

- Gluon-Gluon luminosity ratio

$$\mathcal{R}_{gg}(M, s_2, s_1) \equiv \mathcal{L}_{gg}(M, s_2) / \mathcal{L}_{gg}(M, s_1) \quad (7)$$

- Quark-Gluon luminosity ratio

$$\mathcal{R}_{gq}(M, s_2, s_1) \equiv \mathcal{L}_{gq}(M, s_2) / \mathcal{L}_{gq}(M, s_1) \quad (8)$$

- Quark-Antiquark luminosity ratio

$$\mathcal{R}_{q\bar{q}}(M, s_2, s_1) \equiv \mathcal{L}_{q\bar{q}}(M, s_2) / \mathcal{L}_{q\bar{q}}(M, s_1) \quad (9)$$

- Quark-Quark luminosity ratio

$$\mathcal{R}_{qq}(M, s_2, s_1) \equiv \mathcal{L}_{qq}(M, s_2) / \mathcal{L}_{qq}(M, s_1) \quad (10)$$

In Fig. 3 we show the PDF luminosity ratios, defined as above, for the 8 over 7 TeV ratios and for the 14 over 8 TeV ratios. They have been obtained with NNPDF2.1 NNLO, and the PDF uncertainties have been obtained from the 1000-replica set. PDF errors are computed using 68% Confidence Level intervals to avoid possible non-gaussian behaviors for large final state masses. We also plot in Fig. 3 the percentage PDF errors on these luminosity ratios.

From Fig. 3 we can see that, as well known, the ratio of luminosities increases when the beam energy is increased, growing with the mass of the final state produced particles. This enhancement is a factor between 1.5 and 5 for final states with  $m_X$  between 0.5 and 3 TeV, depending on the dominant partonic subprocesses, and a factor between 2 and 80 in the same range for ratios of 14 over 8 TeV. What is perhaps not so well appreciated is that PDF uncertainties cancel to a very good extent in the ratio, for example, for  $m_X$  below 1.5 TeV the PDF uncertainties in the 8 over 7 TeV luminosity ratio are well below the percent level, confirming the findings of Tables 1–3.

On the other hand, for large invariant masses the cancellation of PDF uncertainties breaks down and PDF errors can become much larger. For the 8 over 7 TeV ratio, for example, the  $q\bar{q}$  luminosity has a very large PDF error, larger than 100%, above  $m_X = 3$  TeV. This is so because in this region one

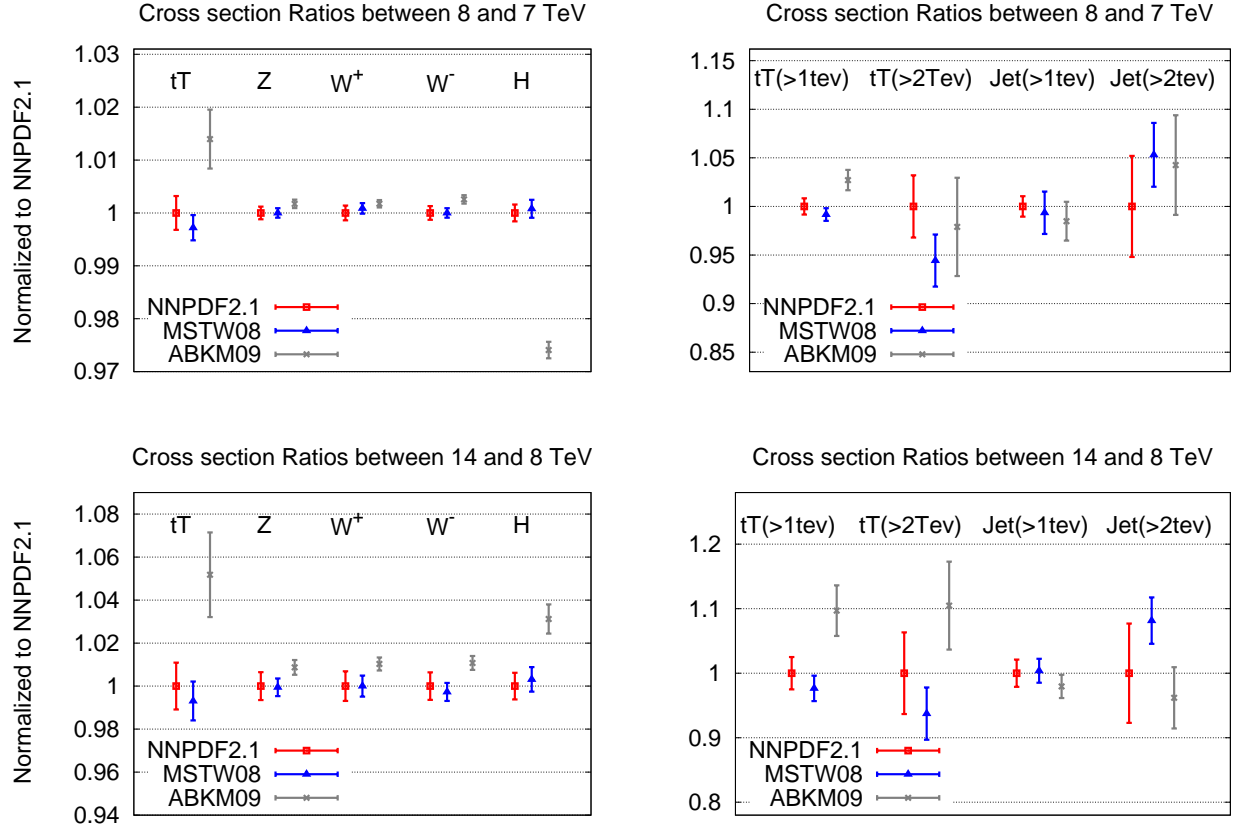


Figure 1: Graphical representation of the results in Tables 4–6 for cross section ratios obtained with different PDF sets. The upper plots show the results for the cross section ratios of 8 over 7 TeV, obtained for all three PDF sets considered for the most relevant observables, normalized to NNPDF2.1 NNLO. The lower plots represent the same ratios this time for 14 over 8 TeV cross sections. The left plot show the results for the inclusive cross sections, which probe  $\mathcal{O}(100 \text{ GeV})$  scales, while the right plots correspond to more differential distributions in the  $\mathcal{O}(1 \text{ TeV})$  region.

is probing the antiquark PDFs at very large  $x$ , a region in which these PDFs are virtually unknown. Is clear thus that the measurement of cross section ratios that involve high mass final states provides stringent constraints on large- $x$  PDFs, which in turn are an important ingredient for new physics searches like supersymmetric particle production [58].

Let us conclude this section by mentioning that the qualitative behavior of the parton luminosity ratios is very similar if the MSTW08 PDF set is used instead.

## 4 Sensitivity to BSM contributions

Having evaluated the systematic uncertainties of the cross section ratios of relevant LHC cross sections, and having seen that they are very small in general, we would like to discuss how the study of these ratios could allow to detect possible Beyond the Standard Model (BSM) contributions, that might be not accessible through absolute cross sections.

If the final state  $X$  receives contributions from both SM and BSM processes, we shall write:

$$\sigma(pp \rightarrow X) = \sigma^{SM}(pp \rightarrow X) + \sigma^{BSM}(pp \rightarrow X) , \quad (11)$$

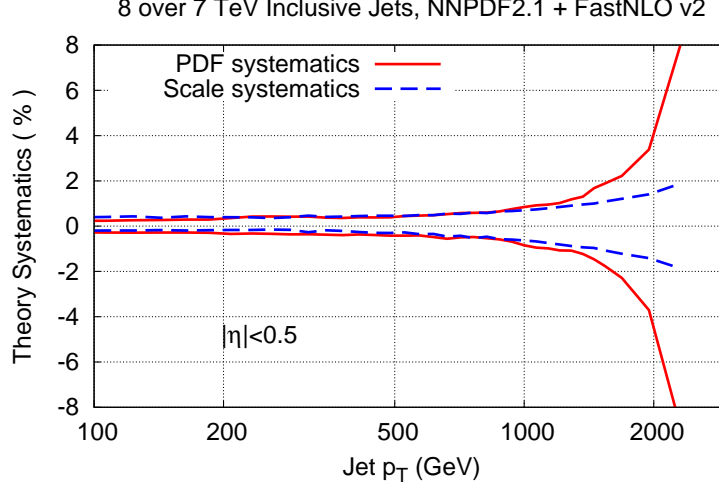


Figure 2: Theory systematics in the 8 over 7 TeV cross section ratios using **FastNLO**. We show the PDF and scale systematics for the ratio of 8 over 7 TeV cross sections for LHC inclusive jet production as a function of the  $p_T$  of the jet, in the central region  $|\eta| \leq 0.5$ .

and, under the assumption that the BSM contamination represents only a small fraction of the total,

$$R_{E_1/E_2}^X \sim \frac{\sigma_X^{\text{SM}}(E_1)}{\sigma_X^{\text{SM}}(E_2)} \times \left\{ 1 + \frac{\sigma_X^{\text{BSM}}(E_1)}{\sigma_X^{\text{SM}}(E_1)} \Delta_{E_1/E_2} \left[ \frac{\sigma_X^{\text{BSM}}}{\sigma_X^{\text{SM}}} \right] \right\}, \quad (12)$$

where we defined, for a quantity  $A$ :

$$\Delta_{E_1/E_2}(A) = 1 - \frac{A(E_2)}{A(E_1)}. \quad (13)$$

The above equations translate in formulas the obvious observation that the visibility of a BSM contribution in the evolution with energy of  $\sigma(X)$  requires that it evolves with energy differently than the SM one: if  $\sigma^{\text{BSM}}(pp \rightarrow X)/\sigma^{\text{SM}}(pp \rightarrow X)$  were independent of  $E$ , no information could be obtained from the study of the energy evolution of  $\sigma(X)$ . The threshold for the visibility of such effects is given by the precision of the SM prediction, which sets the overall theoretical systematics, and defines the goals of the experimental precision:

$$\frac{\sigma_X^{\text{BSM}}(E_1)}{\sigma_X^{\text{SM}}(E_1)} \times \Delta_{E_1/E_2} \left[ \frac{\sigma_X^{\text{BSM}}}{\sigma_X^{\text{SM}}} \right] > \delta_{TH} \equiv \frac{\delta R_{E_1/E_2}^{\text{SM}}}{R_{E_1/E_2}^{\text{SM}}}. \quad (14)$$

Having established in the previous Section that  $\delta_{TH}$  is typically at the percent level, and in some cases at the permille level, BSM contributions of few % could be detected if  $\sigma^{\text{BSM}}(pp \rightarrow X)$  and  $\sigma^{\text{SM}}(pp \rightarrow X)$  have a sufficiently different energy scaling. In addition to the matrix-element structure, which may vary from process to process, the energy scaling depends on the initial state partons ( $i, j$ ), which define the partonic luminosity  $\mathcal{L}_{ij}$ , Eqns. (7–10), as discussed in the previous section.

To give an example, consider the production of a final state  $X$  of mass  $M$ . Assuming that

$$\sigma^{\text{SM}}(X) \sim \mathcal{L}_{ab}(M) \hat{\sigma}^{\text{SM}}(X, M), \quad \sigma^{\text{BSM}}(X) \sim \mathcal{L}_{ij}(M) \hat{\sigma}^{\text{BSM}}(X, M), \quad (15)$$

where the partonic cross sections  $\hat{\sigma}^{\text{SM,BSM}}(X, M)$  depend on  $M$ , but are independent of beam energy, we obtain:

$$\Delta_{E_1/E_2} \left[ \frac{\sigma_X^{\text{BSM}}}{\sigma_X^{\text{SM}}} \right] \sim \Delta_{E_1/E_2} \left[ \frac{\mathcal{L}_{ij}(M)}{\mathcal{L}_{ab}(M)} \right] = 1 - \frac{\mathcal{L}_{ij}(M, E_2)/\mathcal{L}_{ab}(M, E_2)}{\mathcal{L}_{ij}(M, E_1)/\mathcal{L}_{ab}(M, E_1)}. \quad (16)$$

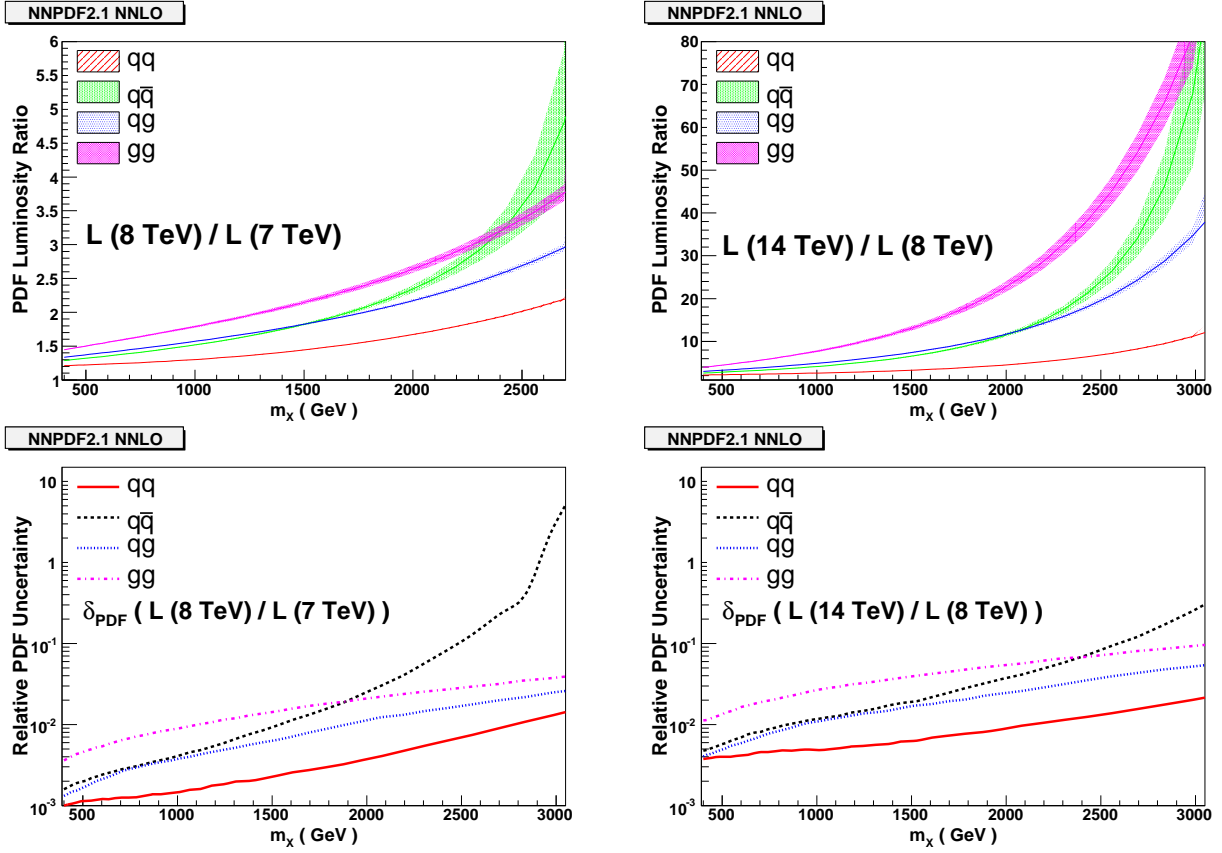


Figure 3: Upper plots: Ratios of PDF luminosities, Eqns. (7–10), between different LHC beam energies. Lower plots: the relative PDF error  $\delta_{\text{PDF}}$  for each of the above luminosity ratios. The left plots show the 8 over 7 TeV ratios while the right plots correspond to the 14 over 8 ratios.

The energy dependence of luminosity ratios could therefore expose the possible existence of BSM phenomena via the study of cross section energy ratios.

We illustrate these considerations with three examples: top quark pair production at large  $t\bar{t}$  pair masses, inclusive jet production at large transverse momentum, and high-mass off-shell  $Z$ -boson production. These processes are dominated by different production channels,  $gg$  for  $t\bar{t}$ ,  $qq$  for jets and  $q\bar{q}$  for  $Z$  production, and are amongst the cross sections that have or will be measured with high precision in the TeV regime, where the sensitivity to new physics is enhanced.

Let's consider first high mass  $t\bar{t}$  production. In this case, the initial state is dominated by  $gg$  fusion. This is shown in Fig. 4, where the left plot gives the fraction of events originated by gluon-gluon collisions, as a function of the minimum value  $M_{t\bar{t}}^{\min}$  of the  $t\bar{t}$  invariant mass  $M_{t\bar{t}}$ , and for different beam energies. The calculation has been done at NLO with the MNR code [44] and the MSTW08 PDFs. We remark that this fraction is largely constant, over a wide range of  $M_{t\bar{t}}$ , in spite of the fact that the  $gg$  luminosity decreases with  $M_{t\bar{t}}$  faster than the  $q\bar{q}$  luminosity. The reason for this behavior is that, while  $\hat{\sigma}_{q\bar{q}}(t\bar{t}) \sim 1/M_{t\bar{t}}^2$ , the  $t$ -channel quark exchange in the  $gg \rightarrow t\bar{t}$  sub-process leads to  $\hat{\sigma}_{gg}(t\bar{t}) \sim \log(M_{t\bar{t}}^2)/M_{t\bar{t}}^2$ . We notice that this behavior remains qualitatively true even requiring the top quarks to be produced in the central rapidity region  $|y_{t,\bar{t}}| < 2.5$ , as shown in the right plot of Fig. 4.

A possible BSM contribution to  $t\bar{t}$  production driven by initial states other than  $gg$ , therefore, would contribute to a deviation from the SM energy scaling of the cross section ratio, as dictated by Eq. (12). For example, in the particular case of a BSM contribution to  $\sigma(t\bar{t})$  due to  $q\bar{q}$  initial states,

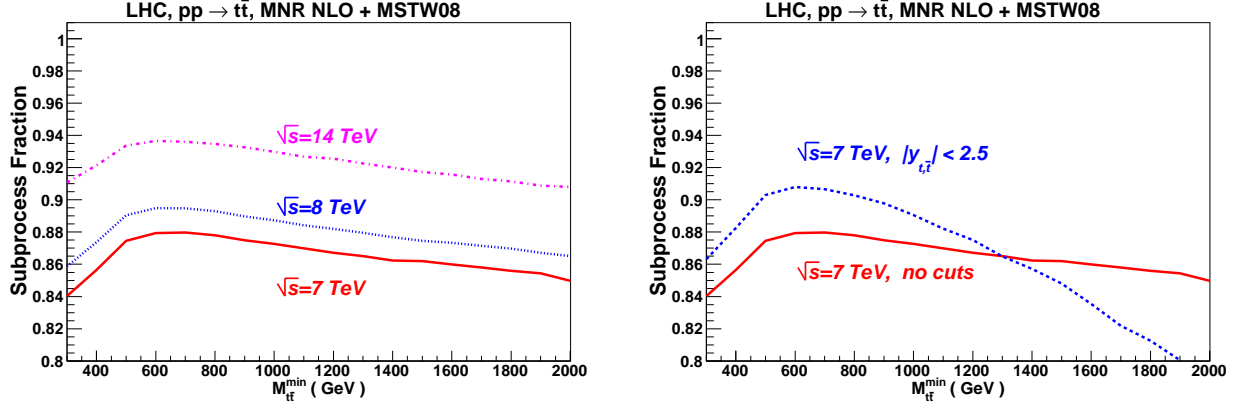


Figure 4: Initial state composition for  $t\bar{t}$  final states, for events with the invariant mass of the top quark pair above a certain threshold,  $M_{t\bar{t}} > M_{t\bar{t}}^{\min}$ , determined at NLO with the MNR code. The left plot shows results for fully inclusive production, at different beam energies. The right plot, at  $\sqrt{s} = 7$  TeV, compares the  $gg$  fraction of fully inclusive final states with the fraction in events with  $|y_t|, |y_{\bar{t}}| < 2.5$ .

as in the case of a  $Z'$  vector boson, the deviation from the SM scaling would be

$$\frac{\sigma_{t\bar{t}}^{\text{BSM}}(E_1)}{\sigma_{t\bar{t}}^{\text{SM}}(E_1)} \Delta_{E_1/E_2} \left[ \frac{\mathcal{L}^{q\bar{q}}(M)}{\mathcal{L}^{gg}(M)} \right] \quad (17)$$

The values of the double ratio of the  $q\bar{q}$  over  $gg$  luminosities at different energies, Eq. (16), is shown in Fig. 5, for ratios of 8 over 7 TeV and 14 over 8 TeV luminosities, computed again from the NNPDF2.1 NNLO PDF set.

From Fig. 5, is clear that for example for a BSM contribution initiated by  $q\bar{q}$ , the enhancement factor due to the different scaling with the energy Eq. (16) could be  $\mathcal{O}(1)$  in most of the TeV region for the 14 over 8 TeV ratios. Given that the systematics in the cross section ratio for top quark pair production at large  $t\bar{t}$  masses is 2-4% at most (and likely to be improved soon), the measurement of this cross section ratio between 14 and 8 TeV should be sensitive to BSM contributions with  $\sigma_{t\bar{t}}^{\text{BSM}}/\sigma_{t\bar{t}}^{\text{SM}}$  well below 10%. For the 8 over 7 ratio the enhancement factor is smaller, but so is the theoretical systematics. This probe is therefore more sensitive to BSM effects than the measurement at a fixed beam energy (unless of course one considers trivially clear BSM signatures such as mass peaks).

For completeness we also show in Fig. 5 the evolution of the luminosity ratios of  $q\bar{q}$  over  $gg$ , and  $qg$  over  $gg$  initial states. We see that in this case there could be a sizable suppression of the cross section ratios for a process whose BSM contribution is quark-quark initiated. Indeed, for 14 over 8 TeV ratios the enhancement factor can be up to  $\mathcal{O}(5)$  for  $m_X \sim 2$  TeV. This means that the ratio of high mass  $t\bar{t}$  cross sections between 14 and 8 TeV can be up to five times more sensitive to BSM  $q\bar{q}$  initiated processes than the absolute cross section, with the cross section prediction and measurement being rather more precise both theoretically and experimentally.

The second illustrative example that we have considered is inclusive jet production. In the case of inclusive jet spectra, the dominant initial state composition varies depending on the jet  $p_T$ . We calculated this, with ALPGEN [59], at leading-order, which is sufficient for our qualitative discussion. The results are shown in fig. 6, which gives the contributions of the  $gg$ ,  $qg$ ,  $q\bar{q}$  and of the quark-quark 'elastic' channel,  $qq^{(\prime)} \rightarrow qq^{(\prime)}$ . At large  $p_T$ , the latter largely dominates, but there is a large range where  $qg$  is also important. The sensitivity of energy ratios of jet spectra to new physics can therefore only be established on a case-by-case basis.

A possible BSM contribution to inclusive jet production at high- $p_T$  driven by a  $q\bar{q}$ ,  $gg$  or  $qg$  initial state, therefore, would contribute to a deviation from the SM energy scaling as dictated from Eq. (12). The values of the double luminosity ratio Eq. (16) for  $q\bar{q}$ ,  $gg$  and  $qg$  luminosities over  $qg$  luminosity are

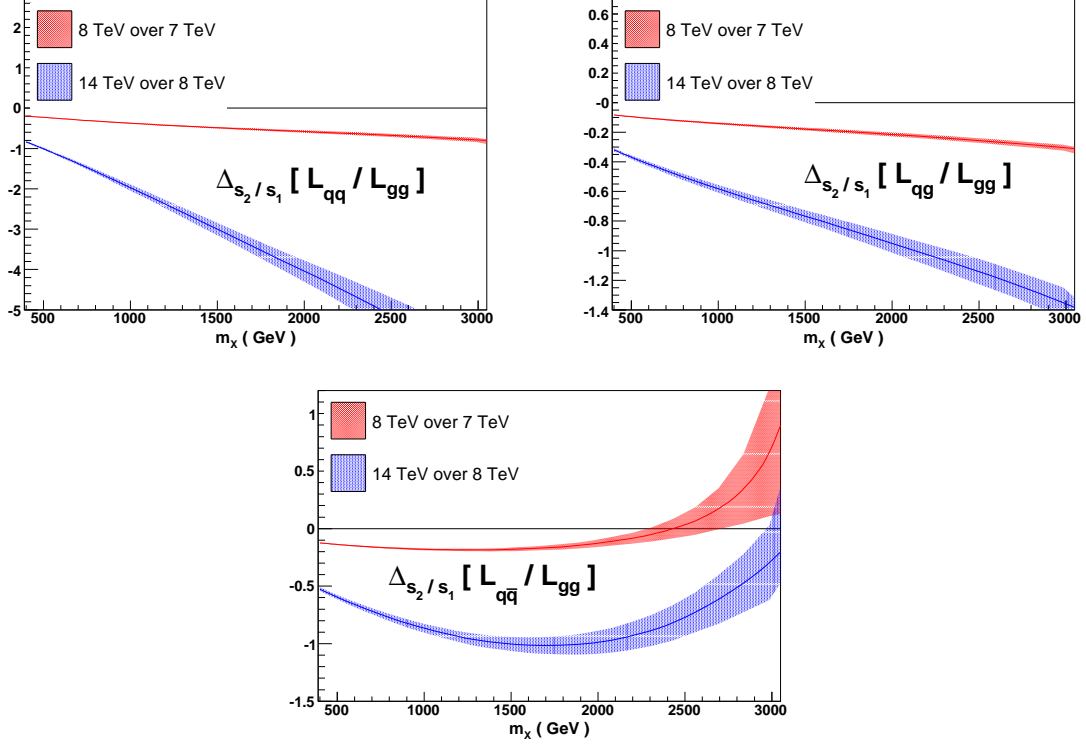


Figure 5: The double ratio of luminosities between different LHC beam energies, Eq. (16) relevant for high mass top quark pair production. The bands correspond to the 1-sigma PDF uncertainties.

represented in Fig. 7, for ratios of 8 over 7 TeV and 14 over 8 TeV luminosities. It is clear that in this case the enhancement of possible BSM contributions is more moderate but still appreciable, reaching  $\mathcal{O}(1)$  at large masses for a  $q\bar{q}$  or  $gg$ -initiated BSM contribution. Thus the measurement of high- $p_T$  jet cross section ratios at different LHC energies, if precise enough, could provide a competitive search strategy for BSM scenarios that lead to the same jet final state.

The final example is high mass off-shell  $Z$  boson production. The initial state composition for high mass Standard Model  $Z$  boson production at the LHC for 7 TeV and 14 TeV, as a function of the invariant mass of the off-shell  $Z$  boson, is shown in Fig. 8. The computation has been done with `Vrap` code at NNLO, with NNPDF2.1 as input. It is clear that the quark-antiquark scattering dominates at all masses, and the  $gg$  contamination is reduced to a few percent.

The double ratios between different LHC beam energies relevant to this case are shown in Fig. 9. For 8 over 7 TeV ratios the scaling with center of mass energy is similar for all luminosities and thus the enhancement of BSM signals is small, except possibly for the highest final state masses where PDF uncertainties explode. For 14 over 8 TeV cross section ratios, instead, the larger lever arm leads to a more important enhancement factor Eq. (16). For example, this can be  $\mathcal{O}(2)$  for BSM  $q\bar{q}$ -initiated contributions, and  $\mathcal{O}(0.5)$  for BSM  $gg$ -initiated contributions.

## 5 Conclusions

We highlighted in this paper the potential interest in precise measurements of ratios and double ratios of cross-sections at different LHC energies. The theoretical precision with which such quantities can be predicted is very high. It can be better than  $10^{-3}$  for electroweak processes, but it is below the percent level even in the case of inclusive  $t\bar{t}$  production, and no larger than a few percent for TeV observables like high mass  $t\bar{t}$  and jet production. Residual theoretical systematics are typically dominated by

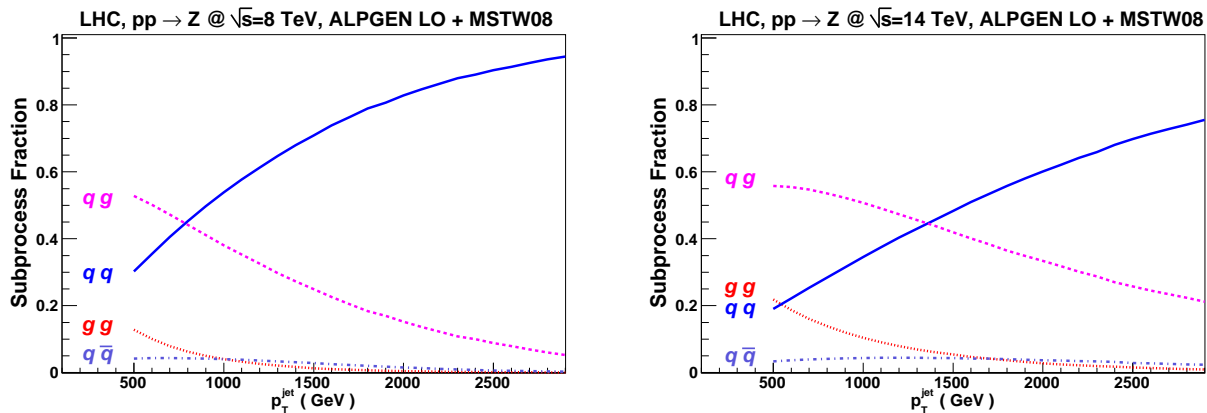


Figure 6: Initial state subprocess fraction for jet final states for 8 TeV (left plot) and 14 TeV (right plot) jet production, as a function of the  $p_T$  of the jet. The computation has been done with ALPGEN at LO. The decomposition of partonic subprocesses is the same as in Eqns. (3–6). The decomposition is very similar between 7 TeV and 8 TeV and thus the 7 TeV case is not shown here.

PDF uncertainties. When these are large enough that the experimental measurements are sensitive to them, the information can be used to improve the knowledge of large- $x$  PDF, a region which is crucial for high mass BSM searches. When these are too small, the relevant ratio can be used as a precise calibration of the relative luminosity of runs at different energies or between different experiments. We also showed that these measurements could expose the presence of small BSM contributions, which may be smaller than the theoretical and experimental systematics at a single energy, but which can alter the energy evolution of the relevant cross sections by a amount larger than the estimated uncertainty and thus be within the reach of the LHC experiments.

The experimental measurements of these ratios and double ratios with the required precision is certainly very challenging, and will require dedicated analyses. Trivial issues, such as generating large enough Monte Carlo statistics to carry out the necessary studies, may also turn out to be possible obstacles. We hope nevertheless that the potential interest in these results, as documented in this note, is compelling enough to stimulate more realistic assessments by the experimental collaborations.

## Acknowledgments

The research of J. R. is supported by a Marie Curie Intra-European Fellowship of the European Community's 7th Framework Programme under contract number PIEF-GA-2010-272515. This work was performed in the framework of the ERC grant 291377, “LHCtheory: Theoretical predictions and analyses of LHC physics: advancing the precision frontier”. We acknowledge the help of K. Rabbertz with FastNLO, J. Gao with MEKS and A. Mitov with top++ .



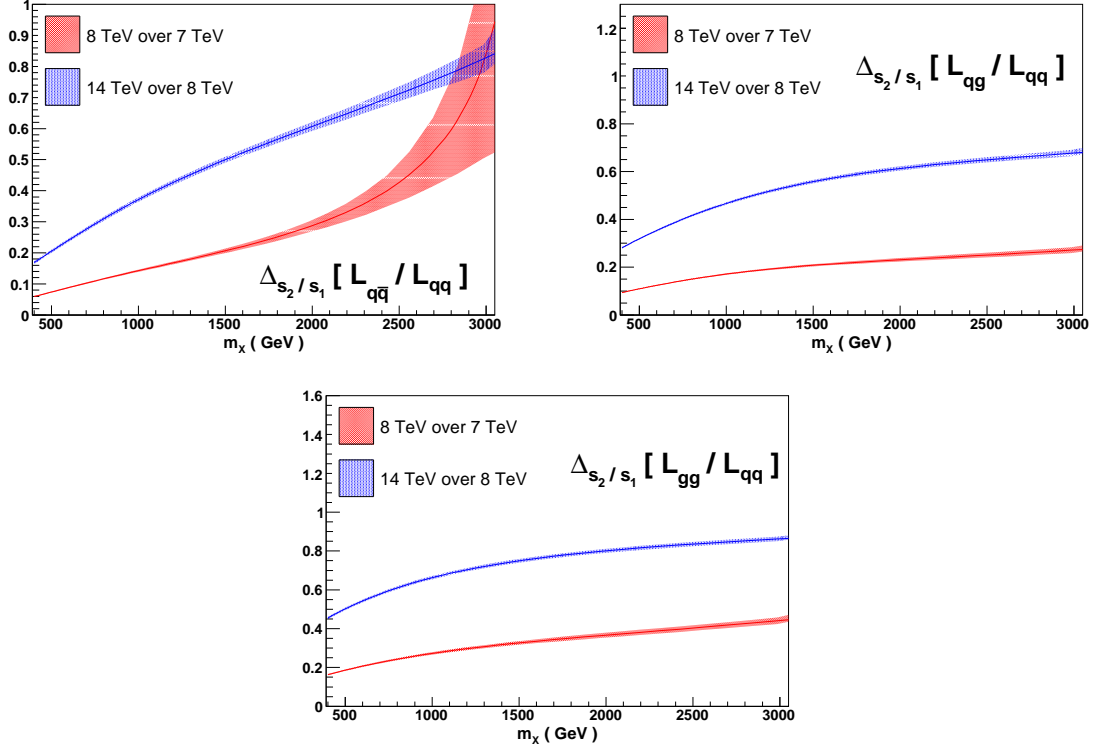


Figure 7: The double ratio of luminosities between different LHC beam energies, Eq. (16) relevant for BSM searches in high  $p_T$  inclusive jet production. The bands correspond to the 1-sigma PDF uncertainties.

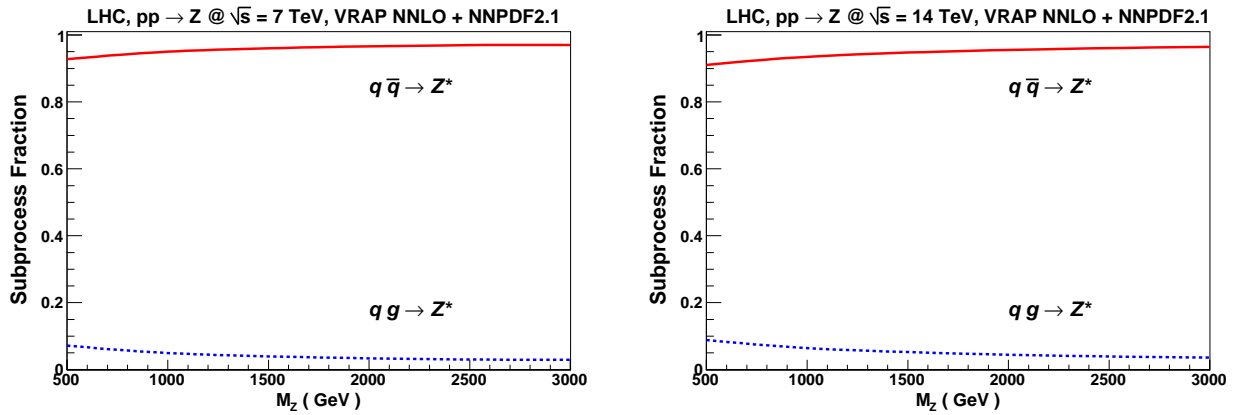


Figure 8: Initial state composition for high mass Standard Model  $Z$  boson production for 7 TeV (left plot) and 14 TeV (right plot) LHC, as a function of the invariant mass of the off-shell  $Z$  boson. The computation has been done with VRAP at NNLO, with NNPDF2.1 as input. The decomposition is very similar between 7 TeV and 8 TeV and thus the latter case is not shown here.

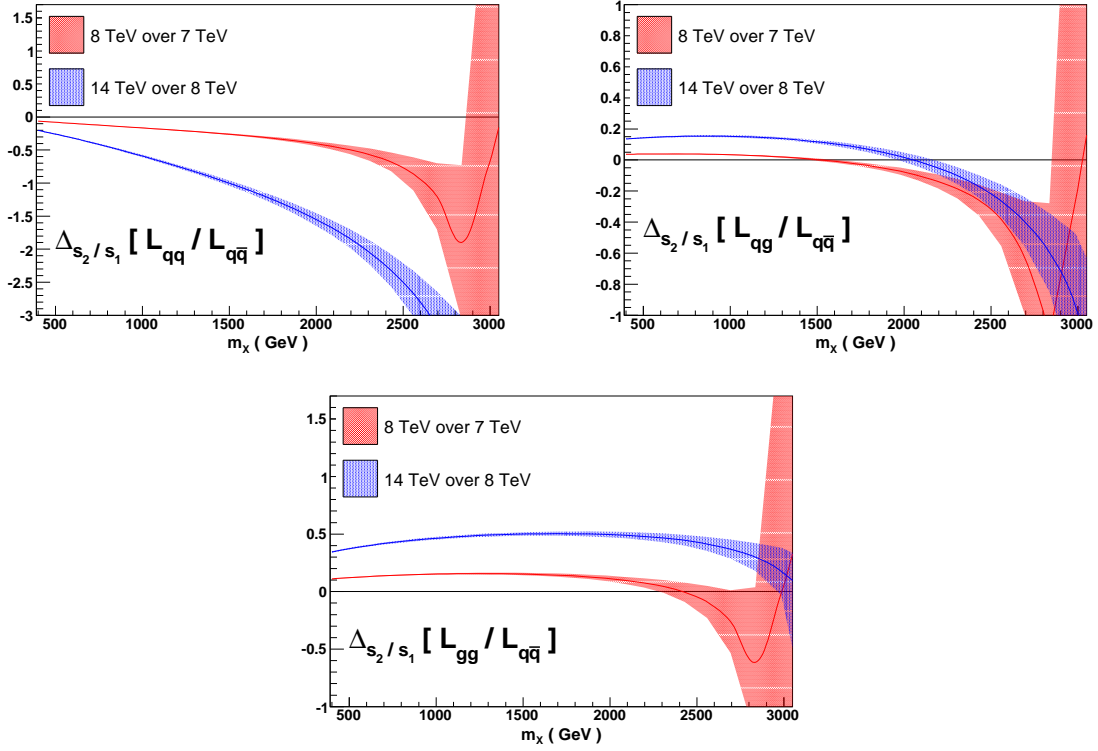


Figure 9: The double ratio of luminosities between different LHC beam energies, Eq. (16) for relevant for BSM searches in high-mass off shell  $Z$  boson production. The bands correspond to the 1-sigma PDF uncertainties.

## References

- [1] CMS Collaboration, S. Chatrchyan et al., Phys.Rev.Lett. 107 (2011) 132001, 1106.0208.
- [2] CMS Collaboration, S. Chatrchyan et al., Phys.Lett. B700 (2011) 187, 1104.1693.
- [3] ATLAS Collaboration, G. Aad et al., (2011), arXiv:1112.6297.
- [4] ATLAS Collaboration, G. Aad et al., JHEP 1205 (2012) 059, arXiv:1202.4892.
- [5] ATLAS Collaboration, G. Aad et al., Phys.Lett. B711 (2012) 244 , arXiv:1201.1889.
- [6] ATLAS Collaboration, G. Aad et al., (2012), arXiv:1205.3130.
- [7] CMS Collaboration, S. Chatrchyan et al., JHEP 1107 (2011) 049, arXiv:1105.5661.
- [8] CMS Collaboration, S. Chatrchyan et al., Phys.Rev.Lett. 107 (2011) 091802, arXiv:1106.3052.
- [9] ATLAS Collaboration, G. Aad et al., Phys.Rev. D85 (2012) 072004, arXiv:1109.5141.
- [10] ATLAS Collaboration, G. Aad et al., Phys.Lett. B701 (2011) 31, 1103.2929.
- [11] CMS Collaboration, S. Chatrchyan et al., (2012), arXiv:1206.2598.
- [12] CMS Collaboration, S. Chatrchyan et al., JHEP 04 (2011) 050, 1103.3470.
- [13] CMS Collaboration, S. Chatrchyan et al., (2011), 1110.4973.
- [14] LHCb Collaboration, R. Aaij et al., (2012), 1204.1620.
- [15] ATLAS Collaboration, G. Aad et al., Phys. Lett. B 706 (2011) 150, 1108.0253.
- [16] CMS Collaboration, S. Chatrchyan et al., Phys.Rev. D84 (2011) 052011, 1108.2044.
- [17] CMS Collaboration, CMS-PAS-EWK-11-013 (2011).
- [18] ATLAS Collaboration, G. Aad et al., Phys.Rev. D85 (2012) 092014, 1203.3161.
- [19] ATLAS Collaboration, G. Aad et al., Phys.Rev. D85 (2012) 092002, arXiv:1201.1276.
- [20] J. A. Maestre et al., arXiv:1203.6803 [hep-ph].
- [21] G. Watt, JHEP 1109 (2011) 069, 1106.5788.
- [22] D. d’Enterria and J. Rojo, Nucl.Phys. B860 (2012) 311, 1202.1762.
- [23] M. Dittmar, F. Pauss and D. Zurcher, Phys.Rev. D56 (1997) 7284, hep-ex/9705004.
- [24] V.A. Khoze et al., Eur.Phys.J. C19 (2001) 313, hep-ph/0010163.
- [25] M. Krasny et al., Eur.Phys.J. C51 (2007) 607, hep-ph/0702251.
- [26] M. Krasny et al., (2011), arXiv:1111.5851.
- [27] M.W. Krasny, Acta Phys.Polon. B42 (2011) 2133, arXiv:1108.6163.
- [28] LHC Lumidays 2012 Workshop, Slides available online at  
<http://indico.cern.ch/conferenceOtherViews.py?view=standard&confId=162948>.
- [29] TOTEM Technical Design Report, CERN-LHCC-2004-002, TOTEM-TDR-001 (2004).

- [30] G. Antchev et al., *Europhys.Lett.* 96 (2011) 21002, arXiv:1110.1395.
- [31] ATLAS Collaboration, “ATLAS Forward Detectors for Measurement of Elastic Scattering and Luminosity”, CERN-LHCC-2008-004, ATLAS-TDR-018 (2008)
- [32] M. Krasny, J. Chwastowski and K. Slowikowski, *Nucl.Instrum.Meth.* A584 (2008) 42, hep-ex/0610052.
- [33] M. Krasny et al., (2010), arXiv:1006.3858.
- [34] V. Budnev et al., *Nucl.Phys.* B63 (1973) 519.
- [35] A. Shamov and V.I. Telnov, *Nucl.Instrum.Meth.* A494 (2002) 51, hep-ex/0207095.
- [36] C. Anastasiou et al., *Phys. Rev.* D69 (2004) 094008, hep-ph/0312266.
- [37] M. Czakon and A. Mitov, (2011), arXiv:1112.5675.
- [38] P. Baernreuther, M. Czakon and A. Mitov, (2012), arXiv:1204.5201.
- [39] M. Cacciari et al., *Phys.Lett.* B710 (2012) 612, arXiv:1111.5869.
- [40] C. Anastasiou et al., *JHEP* 1112 (2011) 058, arXiv:1107.0683.
- [41] D. de Florian and M. Grazzini, *Phys.Lett.* B674 (2009) 291, arXiv:0901.2427.
- [42] J. Campbell and R.K. Ellis, *Phys. Rev.* D65 (2002) 113007, hep-ph/0202176.
- [43] J. Campbell, R.K. Ellis and F. Tramontano, *Phys. Rev.* D70 (2004) 094012, hep-ph/0408158.
- [44] M.L. Mangano, P. Nason and G. Ridolfi, *Nucl.Phys.* B373 (1992) 295.
- [45] Z. Kunszt and D.E. Soper, *Phys. Rev.* D 46 (1992) 192.
- [46] T. Kluge, K. Rabbertz and M. Wobisch, (2006), hep-ph/0609285.
- [47] fastNLO Collaboration, M. Wobisch et al., (2011), arXiv:1109.1310.
- [48] Z. Nagy, *Phys. Rev.* D68 (2003) 094002, hep-ph/0307268.
- [49] The NNPDF Collaboration, R.D. Ball et al., *Nucl. Phys.* B849 (2011) 296, arXiv:1101.1300.
- [50] The NNPDF Collaboration, R.D. Ball et al., *Nucl.Phys.* B855 (2012) 153, arXiv:1107.2652.
- [51] A.D. Martin et al., *Eur. Phys. J.* C63 (2009) 189, arXiv:0901.0002.
- [52] S. Alekhin et al., *Phys. Rev.* D81 (2010) 014032, arXiv:0908.2766.
- [53] S. Bethke, *Eur. Phys. J.* C64 (2009) 689, arXiv:0908.1135.
- [54] F. Demartin et al., *Phys. Rev.* D82 (2010) 014002, arXiv:1004.0962.
- [55] The NNPDF collaboration, R.D. Ball et al., *Nucl. Phys.* B838 (2010) 136, arXiv:1002.4407.
- [56] K. Nakamura et al., PDG collaboration, *Journal of Physics G: Nuclear and Particle Physics* 37 (2010) 075021.
- [57] J.M. Campbell, J.W. Huston and W.J. Stirling, *Rept. Prog. Phys.* 70 (2007) 89, hep-ph/0611148.
- [58] M. Kramer et al., arXiv:1206.2892 (2012).
- [59] M.L. Mangano et al., *JHEP* 0307 (2003) 001, hep-ph/0206293.